Geophysical Research Letters

RESEARCH LETTER
10.1029/2025GL115660

Internal Heat Flux and Energy Imbalance of Uranus

Xinyue Wang[1,2], Liming Li[3], Michael Roman[4], Xi Zhang[5], Xun Jiang[1], Patrick Fry[6], Cheng Li[7], Gwenael Milcareck[8], Agustin Sanchez-Lavega[9], Santiago Perez-Hoyos[9], Ricardo Hueso[9], Tristan Guillot[10], Conor Nixon[11], Ulyana Dyudina[12], Robert West[13], and Matthew Kenyon[13]

[1]Department of EAS, University of Houston, Houston, TX, USA, [2]Now at University of Michigan, Ann Arbor, MI, USA, [3]Department of Physics, University of Houston, Houston, TX, USA, [4]University of Leicester, Leicester, UK, [5]Department of Earth and Planetary Sciences, UCSC, Santa Cruz, CA, USA, [6]University of Wisconsin-Madison, Madison, WI, USA, [7]University of Michigan, Ann Arbor, MI, USA, [8]LMD/IPSL, Sorbonne Universit., PSL Research University, Paris, France, [9]Departamento de Fisica Aplicada I, Escuela de Ingenieria UPV/EHU, Bilbao, Spain, [10]Laboratoire Lagrange, Université Côte d'Azur, CNRS, Nice, France, [11]NASA Goddard Space Flight Center, Greenbelt, MD, USA, [12]Space Science Institute, Boulder, CO, USA, [13]Jet Propulsion Laboratory, California Institute of Technology, Pasadena, CA, USA

Key Points:

- Analyses of Uranus' global radiant energy budget (REB) spanning a complete orbital period (1946–2030) reveal significant seasonal variations
- A statistically significant internal heat flux of 0.078 ± 0.018 Wm^{-2} is determined from long-term investigations of Uranus REB
- Large energy imbalances at both global and hemispheric scales are suggested for Uranus' weather layer

Supporting Information:

Supporting Information may be found in the online version of this article.

Correspondence to:

L. Li,
lli7@central.uh.edu

Citation:

Wang, X., Li, L., Roman, M., Zhang, X., Jiang, X., Fry, P., et al. (2025). Internal heat flux and energy imbalance of Uranus. *Geophysical Research Letters*, *52*, e2025GL115660. https://doi.org/10.1029/2025GL115660

Received 3 MAR 2025
Accepted 13 JUN 2025

Author Contributions:

Conceptualization: Liming Li, Xun Jiang
Data curation: Liming Li, Xun Jiang
Formal analysis: Xinyue Wang, Liming Li, Michael Roman, Xi Zhang, Xun Jiang, Patrick Fry, Cheng Li, Gwenael Milcareck, Agustin Sanchez-Lavega, Santiago Perez-Hoyos, Ricardo Hueso, Tristan Guillot, Conor Nixon, Ulyana Dyudina, Robert West, Matthew Kenyon
Funding acquisition: Liming Li, Xun Jiang
Investigation: Liming Li, Xun Jiang, Cheng Li
Methodology: Liming Li, Xun Jiang
Project administration: Liming Li, Xun Jiang

Abstract With its extreme axial tilt, Uranus' radiant energy budget (REB) and internal heat flux remain among the most intriguing mysteries in our solar system. By combining observations with modeling, we present the global REB over a complete orbital period (1946–2030), revealing significant seasonal variations. Despite these fluctuations, the global average emitted thermal power consistently exceeds absorbed solar power, indicating a net energy loss. Assuming no significant seasonal variation in emitted power, we estimate an internal heat flux of 0.078 ± 0.018 W/m^2 by analyzing the energy budget over one orbital period. The combination of internal heat and radiant energies indicates substantial global and hemispheric imbalances, with excesses or deficits exceeding 85% of emitted power at the hemispheric scale. These findings are crucial for understanding Uranus' interior and atmosphere. A future flagship mission to Uranus would provide critical observations to address more unresolved questions of this enigmatic ice giant.

Plain Language Summary The study of radiant energy budgets and internal heat is crucial in astronomy, planetary science, and atmospheric science, as it helps us understand planetary weather, climate dynamics, and the processes governing planetary formation and evolution. Uranus, with its extreme axial tilt and enigmatic energy balance, presents a particularly compelling case. In this study, we present the global-average radiant energy budget spanning a complete orbital period (1946–2030) based on observations and modeling, revealing significant seasonal variations driven primarily by Uranus' highly variable solar flux. Despite these fluctuations, our results show that emitted thermal power consistently exceeds absorbed solar power, indicating a net energy loss. From these seasonal variations, we determine a statistically significant internal heat flux, resolving the long-standing debate on its magnitude. Furthermore, we analyze the energy budget of Uranus' weather layer by integrating internal heat with radiant energies, uncovering substantial energy imbalances at both global and hemispheric scales. This is the first study to quantify seasonal energy imbalances on Uranus. Our findings provide critical insights into the planet's thermal dynamics for future investigations, including those by a potential flagship mission to Uranus.

1. Introduction

As an ice giant, Uranus has garnered special attention due to its unique obliquity and extremely strong seasonal variations. Compared to the gas giants Jupiter and Saturn, Uranus and its fellow ice giant, Neptune, have been visited by relatively few spacecraft, partly due to their long distance from Earth. This scarcity of observations is one of the main motivations behind the proposed flagship mission to Uranus, which has been ranked as the highest priority in NASA's planetary science program for the next decade, as reported in the Decadal Strategy for Planetary Science and Astrobiology 2023–2032 from the National Academies of Sciences, Engineering, and Medicine (2022).

The Voyager spacecraft, along with ground-based telescopes and Earth-orbiting observatories, has significantly enhanced our understanding of Uranus. However, many mysteries about this ice giant remain. In this study, we examine the radiant energy budget (REB) and internal heat flux of Uranus. The balance or imbalance between absorbed solar energy and emitted thermal energy, known as the REB, plays a crucial role in determining Uranus'

Resources: Liming Li, Xun Jiang
Software: Liming Li
Supervision: Liming Li, Xun Jiang, Cheng Li
Validation: Liming Li, Xun Jiang
Visualization: Xinyue Wang
Writing – original draft: Xinyue Wang
Writing – review & editing: Liming Li, Michael Roman, Xi Zhang, Xun Jiang, Patrick Fry, Cheng Li, Gwenael Milcareck, Agustin Sanchez-Lavega, Santiago Perez-Hoyos, Ricardo Hueso, Tristan Guillot, Conor Nixon, Ulyana Dyudina, Robert West, Matthew Kenyon

thermal properties (e.g., Conrath et al., 1989; R. A. Hanel et al., 2003). This budget also regulates energy transfer and conversion within Uranus' atmospheric system, influencing its atmospheric dynamics and weather patterns. Giant planets are internally hot, a property tied to their formation and evolution. An internal heat flux results both from the slow release of this internal heat and from other energy sources such as radioactivity or phase separations (e.g., Flasar, 1973; Guillot, 2005; Hubbard, 1968; Salpeter, 1973; Smoluchowski, 1967; Stevenson & Salpeter, 1977). Although directly measuring internal heat flux is challenging, the REB provides an indirect yet essential method for estimating this property (e.g., Conrath et al., 1989).

A recent study (Wang et al., 2024) suggests that seasonal variations must be considered when investigating the REBs and internal heat flux of giant planets. Among all planets in our solar system, Uranus is expected to exhibit the strongest seasonal variations in solar flux and the associated REB, due to its unique obliquity (97.77°) and notable orbital eccentricity (0.047). These seasonal REB variations not only drive temporal changes in Uranus' atmospheric system but also play a critical role in determining its internal heat flux. However, studying Uranus' seasonal REB variations is challenging due to its long orbital period (∼84 years) and extended seasonal durations (∼20–22 years). Consequently, these variations remain largely unexplored, primarily due to the lack of long-term observations.

This limitation further complicates efforts to assess the planet's internal heat flux. Although microwave observations of Uranus' interior thermal structure suggest the presence of internal heat (Gulkis & de Pater, 1984), the magnitude of the internal heat flux has long been debated and remains poorly constrained. Observational analyses suggest that Uranus does not exhibit statistically significant internal heat flux (e.g., Pearl et al., 1990; Pollack et al., 1986), whereas detailed modeling and theoretical examination indicate that it should (e.g., Ge et al., 2024; Marley & McKay, 1999). Since other giant planets (i.e., Jupiter, Saturn, and Neptune) exhibit significant internal heat flux (Conrath et al., 1989; R. A. Hanel et al., 2003; Ingersoll, 1990; Li et al., 2018; Pearl & Conrath, 1991; Wang et al., 2024), resolving this discrepancy for Uranus is crucial. Determining whether Uranus has internal heat flux would provide key insights into the formation and evolution of giant planets.

2. Methodology

Fortunately, many more observations have become available since the early studies, which were primarily based on Voyager data from the 1980s (Pearl et al., 1990; Pollack et al., 1986). In this study, we utilize Voyager data along with more recent observations to re-examine Uranus' REB and its seasonal variations, as well as to determine its internal heat flux. The detailed process of how the REB is measured based on available observations and studies are provided in (Figures S1–S19 in Supporting Information S1). Here, we briefly introduce the process. The basic methodology and observational data are summarized in Sections S1 and S2 in Supporting Information S1, respectively. This study emphasizes two key aspects: (a) seasonal variations and (b) analysis at both global and hemispheric scales. To examine a full seasonal cycle of Uranus' REB, we must consider an entire orbital period (∼84 years). Modern observational records of Uranus date back to the 1950s. Therefore, we select the period from 1946 to 2030, which encompasses the available observations from 1950 to 2022. The observational period from 1950 to 2022 covers approximately 87% of a complete Uranian year (1946–2030), and modeling based primarily on symmetry arguments is used to fill the remaining gaps in temporal coverage (see Section S3 in Supporting Information S1). Uranus' REB is determined by two components: absorbed solar energy and emitted thermal energy. Absorbed solar power is generally calculated using the incident solar power at Uranus (i.e., the solar flux) and the Bond albedo. The reflected solar power from the sunlit disk (Figure S1 in Supporting Information S1), which exhibits different latitudinal coverage in different seasons, can be combined with the incident solar power (Figures S2–S5 in Supporting Information S1) to determine the Bond albedo. Investigations of Uranus' Bond albedo and the corresponding absorbed solar power at global and hemispheric scales over a complete Uranian year (1946–2030) are presented in Section S4 in Supporting Information S1 (Figures S6–S13 in Supporting Information S1). Uranus' emitted power at both global and hemispheric scales for the same period is discussed in Section S5 in Supporting Information S1 (Figures S14–S18 in Supporting Information S1). Finally, we examine Uranus' REB, particularly in its two hemispheres, namely the Northern Hemisphere (NH) and the Southern Hemisphere (SH), in Section S6 in Supporting Information S1 (Figure S19 in Supporting Information S1).

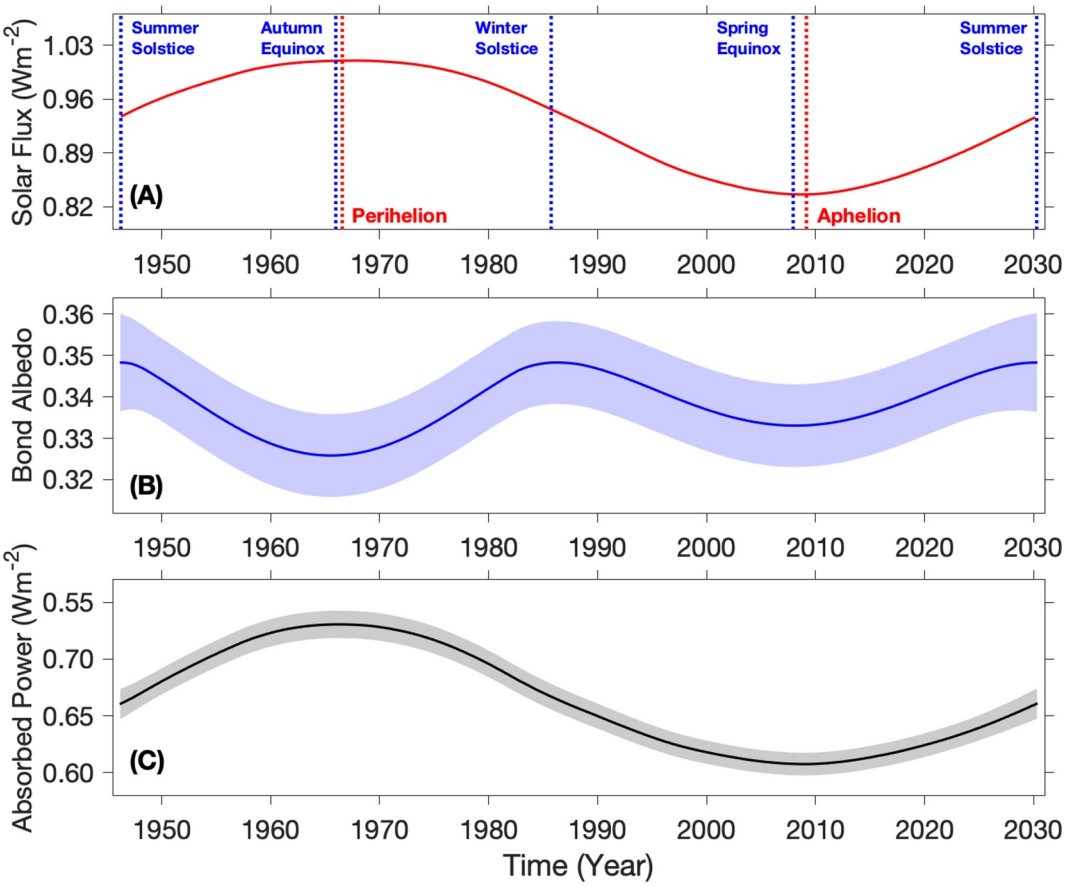

Figure 1. Solar flux, Bond albedo, and absorbed solar power during Uranus' orbital period from 1946 to 2030. (a) Global-average solar flux at Uranus. (b) Disk-average Bond albedo for the sunlit disk. (c) Global-average absorbed solar power. In panel a, the five blue vertical dashed lines mark the summer and winter solstices, as well as the spring and autumn equinoxes of the Northern Hemisphere. The two red vertical dashed lines represent Uranus' perihelion and aphelion in its orbit around the Sun. The shaded regions in panels b and c indicate uncertainties in measurements. The time series of Bond albedo shown in panel b is derived from the seasonal variations in disk-averaged reflectivity at blue and yellow wavelengths (Figure S6 in Supporting Information S1), a more complete spectral coverage of geometric albedo (Figure S7 in Supporting Information S1), and a re-examination of the phase function (Figure S9 in Supporting Information S1) (see Section S4 in Supporting Information S1 for a detailed discussion).

3. Results

Figure 1 presents the solar flux, Bond albedo, and absorbed solar power at the global scale. Uranus' relatively high orbital eccentricity causes the Sun-Uranus distance to increase by ∼10.0% from perihelion in 1966 to aphelion in 2009, leading to a corresponding ∼16.8% decrease in solar flux, from ∼1.01 Wm^{-2} at perihelion to ∼0.84 Wm^{-2} at aphelion (Figure 1a). Figure 1b indicates that the disk-averaged Bond albedo exhibits periodic variations. It is worth noting that the actual seasonal variations of Uranus' Bond albedo could be more complex than the periodic variations derived from fitting the observations with periodic functions.

Figure 1b suggest that the Bond albedo reaches maxima near the summer and winter solstices (1946, 1985, and 2030) and minima around the spring and autumn equinoxes (1966 and 2007) of each hemisphere. These variations likely result from both spatial differences in albedo (e.g., brighter polar regions compared to lower latitudes) (e.g., P. G. J. Irwin et al., 2011, P. G. Irwin et al., 2024; Karkoschka, 2001; G. Lockwood, 1978; G. W. Lockwood, 2019; G. W. Lockwood and Jerzykiewicz, 2006) and seasonal changes in albedo (e.g., Hammel & Lockwood, 2007; Rages et al., 2004). The disk-average Bond albedo varies by ∼6.3%, from a maximum of ∼0.348 during the summer and winter solstices (1946, 1985, and 2030) to a minimum of ∼0.326 during the autumn equinox (1966) of each hemisphere. Since seasonal variations in solar flux are stronger than those in Bond albedo, the seasonal pattern of the global-average absorbed solar power (Figure 1c) closely follows that of solar

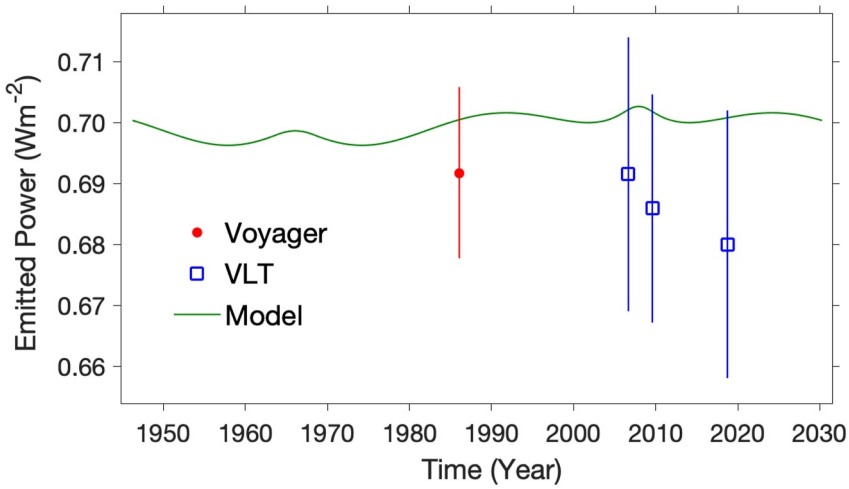

Figure 2. Global-average emitted power of Uranus. The most accurate measurement based on Voyager observations in 1986 (Pearl et al., 1990) is shown as a red dot. New estimates of global-average emitted power for three years (2006, 2009, and 2018), derived from brightness temperature observations recorded by the Very Large Telescope (Orton et al., 2015; Roman et al., 2020), are represented by blue squares. The global-average emitted power obtained from numerical simulations of Uranus' atmosphere (Wallace, 1983) is shown as a green line. The vertical lines for the Voyager and VLT results indicate measurement uncertainties.

flux. Figure 1c further suggests that global-average absorbed power decreases by 18.2% ± 2.0%, from 0.681 ± 0.011 Wm^{-2} around perihelion to 0.557 ± 0.008 Wm^{-2} around aphelion.

Now, we discuss the other component of the REB: the emitted power. Figure 2 presents the best measurement of Uranus' global-average emitted power based on Voyager observations (Pearl et al., 1990), along with our estimates derived from Uranus' brightness temperature observations (see Section S5 in Supporting Information S1). Additionally, Figure 2 includes the global-average emitted power obtained from numerical simulations of Uranus' atmosphere (Wallace, 1983). First, the differences in emitted power between the Voyager measurement (0.692 ± 0.014 Wm^{-2} in 1986) and our estimates from brightness temperature (0.692 ± 0.022 Wm^{-2}, 0.686 ± 0.019 Wm^{-2}, and 0.680 ± 0.022 Wm^{-2} for 2006, 2009, and 2018 respectively) are smaller than their respective uncertainties, suggesting that temporal variations in Uranus' global-average emitted power are not statistically significant. The numerical simulations (Wallace, 1983) also show relatively small seasonal variations in the global-average emitted power, with a ratio of the standard deviation of seasonal variations to the annual mean of ∼0.3%.

A comparison between the simulated emitted power and the best measurement from Voyager (Pearl et al., 1990) shows that the difference between them is smaller than the measurement uncertainty, indicating that the simulation and measurement are statistically consistent. More importantly, the seasonal variation in the simulated emitted power is smaller than the uncertainty of the Voyager measurement, further supporting the conclusion that Uranus' global-average emitted power does not exhibit significant seasonal variations. The radiative time constant of Uranus' upper troposphere and lower stratosphere is longer than 160 years (e.g., Allison & Travis, 1986; Conrath et al., 1990; R. Hanel et al., 1986), which exceeds its orbital period. The long radiative time contributes to the relatively weak seasonal variations in the large-scale thermal structure of Uranus' atmosphere (e.g., Bézard, 1990; Bezard & Gautier, 1985; Conrath et al., 1990; Friedson & Ingersoll, 1987; Milcareck et al., 2024; Orton et al., 2015; Roman et al., 2020; Wallace, 1983). Because the thermal structure is closely related to emitted power, these weak seasonal variations in thermal structure help explain the insignificant seasonal variations in Uranus' global-average emitted power.

In summary, both observations and simulations indicate that Uranus' global-average emitted power does not show statistically significant seasonal variations. Therefore, we assume it remains constant with season and adopt the best measurement from Voyager (0.692 ± 0.014 Wm^{-2}) as the time-invariant value for our subsequent analysis of seasonal variations in the global-average REB and the reexamination of the internal heat flux. It should be noted that Uranus' actual emitted power may exhibit some degree of seasonal variations, even if such variations are not

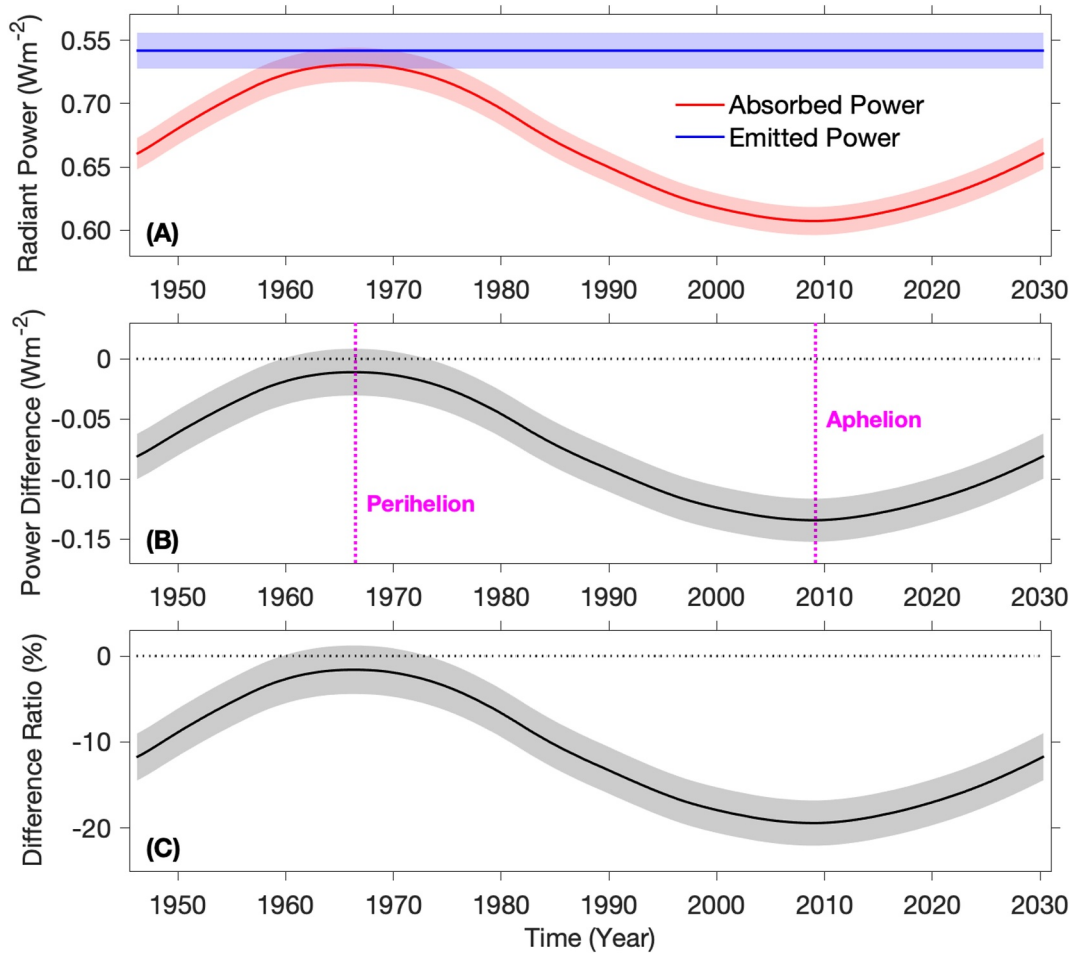

Figure 3. Uranus' global-average absorbed power, emitted power, and their difference. (a) Comparison between global-average absorbed solar power and emitted thermal power. (b) Difference between absorbed and emitted powers (i.e., absorbed power minus emitted power). (c) Ratio of this difference to emitted power. The shaded regions in all three panels indicate uncertainties. The two magenta vertical dashed lines in panel b mark Uranus' perihelion and aphelion in its orbit around the Sun. In panels b and c, the black horizontal dashed lines represent zero difference, serving as a reference.

very pronounced. These potential seasonal variations can affect the annual-mean emitted power, which is used to estimate the internal heat flux (see discussion below). In other words, the uncertainty in the annual-mean emitted power may be larger than the uncertainty of emitted power estimated from the Voyager measurements (0.014 W/m^2) if seasonal variability is taken into account.

To determine Uranus' REB and its seasonal variations, we compare absorbed solar power and emitted thermal power from 1946 to 2030, as shown in Figure 3. Panel a suggests that emitted thermal power exceeds absorbed solar power throughout Uranus' orbital period. Panel b shows that the difference between absorbed and emitted powers (i.e., absorbed power - emitted power) follows a similar pattern to absorbed solar power, since Uranus' global-average emitted power remains constant within measurement uncertainty (Figure 2). This difference ranges from 0.011 ± 0.019 Wm^{-2} at perihelion in 1966 to 0.134 ± 0.018 Wm^{-2} around aphelion in 2009. Correspondingly, the ratio of this power difference to emitted power increases from 1.6% ± 2.8% in 1966 to 19.4% ± 2.6% in 2009 (Figure 3, Panel C). Taking absorbed solar power as a reference, the ratio is even higher, rising from 1.63% ± 2.87% at perihelion to 24.10% ± 3.26% at aphelion.

For Uranus, the fact that emitted thermal power exceeds absorbed solar power indicates a radiant energy deficit, implying that Uranus is losing energy, though the cause and consequences of this energy loss are not yet fully understood. The difference between absorbed and emitted powers can be used to estimate internal heat flux (e.g., Conrath et al., 1989; R. A. Hanel et al., 2003). Previous estimates of Uranus' internal heat flux have not fully

accounted for seasonal variations in the REB, leading to less precise estimates. This omission has contributed to discrepancies in past studies regarding whether Uranus has internal heat flux (Ge et al., 2024; Marley & McKay, 1999; Pearl et al., 1990; Pollack et al., 1986). Here, we re-examine Uranus' internal heat flux by accounting for seasonal variations in the radiant energy budget (REB) and further assume that the difference between the average emitted and absorbed powers over a complete Uranian year can be used to estimate the internal heat flux.

Here, we assume that Uranus' internal heat flux does not have seasonal variations. Figure 3 shows that the difference between absorbed and emitted power varies across seasons, indicating that the power difference in any given season does not accurately represent Uranus' internal heat flux, which operates on much longer timescales. To estimate the internal heat flux, we average the power difference over a complete Uranian year, yielding a value of 0.078 ± 0.018 W/m^2. The corresponding annual-mean absorbed and emitted powers are 0.614 ± 0.012 W/m^2 and 0.692 ± 0.014 W/m^2, respectively. The ratio of annual-mean emitted to absorbed power is 1.13 ± 0.03. Furthermore, Uranus' internal heat flux accounts to $12.52\% \pm 0.31\%$ of the absorbed solar power and $11.13\% \pm 0.27\%$ of the emitted thermal power.

Thus, we conclude that Uranus does have internal heat flux, although the ratio of internal heat flux to absorbed solar power (12.52%) is significantly lower than those of other giant planets (i.e., 113%, 139%, and 162% of absorbed solar power for Jupiter, Saturn, and Neptune, respectively) (Li et al., 2018; Pearl & Conrath, 1991; Wang et al., 2024). Various theories have been proposed to explain Uranus' relatively low internal heat flux, including hypotheses regarding its interior structure and evolutionary history (Hubbard, 1978, 1980; Podolak et al., 1991). The seasonal variations in the REB and new measurements of internal heat flux presented here provide additional constraints and insights to refine models of Uranus' interior and evolutionary processes.

The internal heat flux also plays an important role in the atmospheric systems of giant planets. It is one of the driving forces of the weather layer of giant planets, which is defined as the upper troposphere including clouds. For Uranus' weather layer, which ranges from the tropopause at ~100 mbar (West et al., 1991) to the lower boundary near the water clouds at ~200 bars (Allison et al., 1991; Allison & Travis, 1986), we can combine the seasonally varying absorbed solar power and the internal heat flux (0.078 ± 0.018 Wm^{-2}) as the input power. In contrast, the output power is determined solely by the emitted thermal power.

Panel a of Figure 4 compares the input and output powers on a global scale, revealing a significant energy imbalance. The global-average energy imbalance ranges from an excess of $9.5\% \pm 3.5\%$ of the emitted power at perihelion in 1966 to a deficit of $-8.3\% \pm 3.3\%$ of the emitted power at aphelion in 2009. Figure 4 also shows that the global-average energy excess primarily occurs in the two seasons around perihelion (i.e., summer and autumn in the NH), while the global-average energy deficit mainly appears in the two seasons around aphelion (i.e., winter and spring in the NH). The strong seasonal variations in absorbed flux, which far exceed the trivial seasonal variations of the nearly season-constant emitted power, result in a global average seasonal energy imbalance.

Uranus' extreme axial tilt (97.7°) is expected to cause pronounced seasonal variations in the hemispheric-average energy budget. Therefore, we also examine the energy budget of the weather layer at the hemispheric scale. Assuming that the internal heat flux does not differ between hemispheres, we use the global-average internal heat flux to approximate the hemispheric-average internal heat flux. Then we can combine the hemispheric-average internal heat flux with the hemispheric REB (Figure S19 in Supporting Information S1) to examine the energy budget of the weather layer at the hemispheric scale. Panels b and c of Figure 4 illustrate the hemispheric energy budget of Uranus' weather layer, which exhibits extreme energy imbalances on a seasonal scale. The two hemispheres experience completely opposite energy imbalances at the solstices: one hemisphere undergoes an extreme energy excess, while the other experiences a significant energy deficit. The ratio of the hemispheric-average power difference (i.e., input power–output power) to output power varies substantially, from $95.0\% \pm 6.7\%$ at the summer solstice to $-87.7\% \pm 3.9\%$ at the winter solstice in each hemisphere. If we take the input power as reference, the energy deficit at the winter solstice of each hemisphere can reach $\sim -713.1\% \pm 164.3\%$ of the input power.

Although the two hemispheres experience entirely opposite energy imbalances at the solstices (Figure 4), the thermal structure of Uranus' upper troposphere and lower stratosphere does not exhibit a pronounced asymmetry between them (e.g., Conrath et al., 1990; Orton et al., 2015; Pearl & Conrath, 1991; Roman et al., 2020). Therefore, a mechanism is required to transport solar heating from the sunlit hemisphere to the other hemisphere

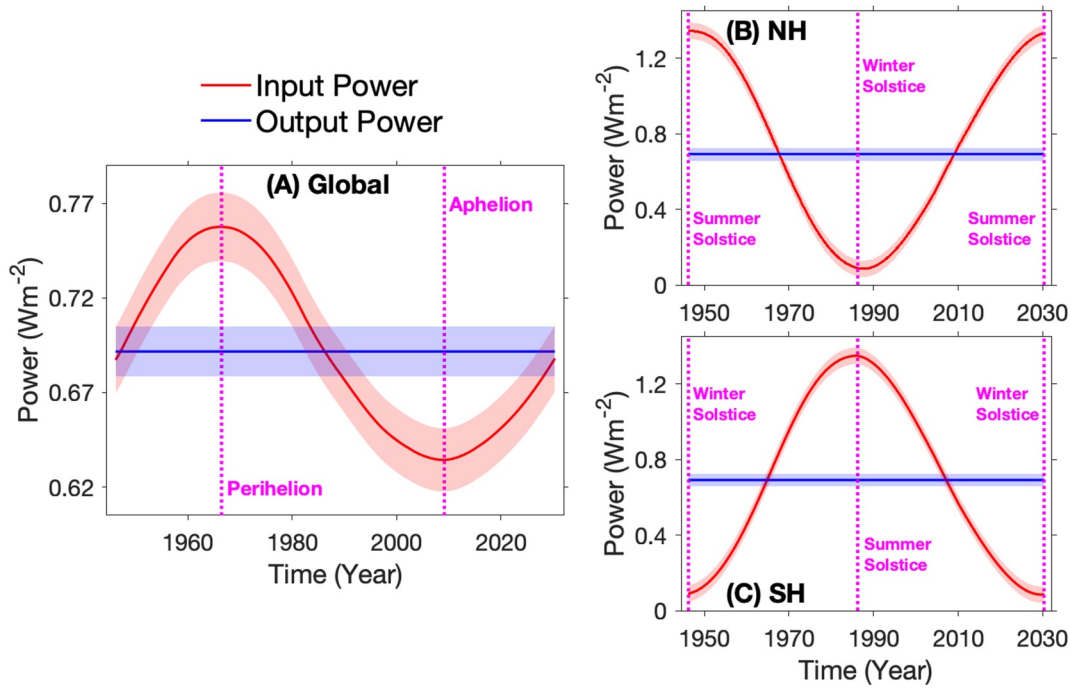

Figure 4. Energy budget of Uranus' weather layer at global and hemispheric scales. (a) Comparison of global-average input and output powers. (b) and (c) show the same comparison as (a) but for the Northern Hemisphere and Southern Hemisphere, respectively. The input power is determined by combining the absorbed solar power with the internal heat flux, as described in the text. The output power is derived solely from the emitted thermal power. In panel a, the two magenta vertical dashed lines indicate Uranus' perihelion and aphelion in its orbit around the Sun. In panels b and c, the magenta vertical dashed lines mark the summer and winter solstices for the respective hemisphere. The shaded regions in all three panels represent uncertainties.

during solstices, possibly related to meridional circulation in the upper atmosphere (e.g., Friedson & Ingersoll, 1987). The quantitative characteristics of energy imbalance at both global and hemispheric scales can help constrain the mechanisms responsible for solar heating transport on Uranus.

4. Conclusion and Discussion

In this study, Uranus' Bond albedo is determined by measuring the geometric albedo across a complete wavelength range and re-examining the phase function. The Bond albedo measurements are then used to determine seasonal variations in absorbed solar power. Seasonal variations in Uranus' emitted power are also examined through both observations and simulations. Based on these measurements, we provide the global-average picture of Uranus' REB over a complete orbital period (1946–2030). While the thermal structure and emitted power exhibit little seasonal variation due to the long radiative timescale, the global-average REB undergoes significant seasonal changes, primarily driven by Uranus' strongly variable seasonal solar flux. Despite these fluctuations, the emitted thermal power consistently exceeds the absorbed solar power, indicating that Uranus is losing energy.

Seasonal variations in the REB, which were not fully accounted for in previous estimates, enable a more accurate determination of Uranus's internal heat flux. Our new analysis yields a statistically significant value of 0.078 ± 0.018 Wm^{-2}, corresponding to $12.52\% \pm 0.31\%$ of the absorbed solar power. This demonstrates the positive net value of the heat flux, close to Voyager 2's upper limit and in line with predictions from detailed radiative transfer models (Ge et al., 2024; Marley & McKay, 1999). The ratio of internal heat flux to absorbed solar power remains, however, significantly lower than for Jupiter, Saturn, and Neptune. The heat flux, expressed in luminosity per unit mass, is 7.3×10^{-12} W kg^{-1}, slightly exceeding the value of 5.2×10^{-12} W kg^{-1} for carbonaceous chondrites (Clauser, 2021). Given that rocks account for less and possibly well below 50% of Uranus's mass (Malamud et al., 2024), and that the remaining components contribute negligibly to radioactive heating, we conclude that the internal heat flux we measure reflects Uranus's ongoing cooling. The fact that this value is about an order of magnitude smaller than that for Neptune remains to be accounted for.

The quantitative characteristics of Uranus' internal heat flux provide observational constraints that can be used to develop theories of planetary formation for giant planets, including Uranus. For Uranus' atmosphere, previous numerical models either omitted internal heat flux or incorporated it with imprecise values (e.g., Bézard, 1990; Bezard & Gautier, 1985; Conrath et al., 1990; Friedson & Ingersoll, 1987; Milcareck et al., 2024; Wallace, 1983). The new measurements of internal heat flux offer a basis for re-evaluating these atmospheric models.

Some theoretical studies (Bézard, 1990; Bezard & Gautier, 1985; Friedson & Ingersoll, 1987; Wallace, 1983) suggest that internal heat flux may vary with latitude and season if it is associated more with the weather layer rather than originating from the planet's deep interior. If we define the difference between absorbed and emitted powers at any given time as instantaneous internal heat flux, we find that the global-scale instantaneous internal heat flux varies from 1.60% ± 2.82% of the emitted power at perihelion to 19.42% ± 2.63% at aphelion. The hemispheric-scale REB suggests that instantaneous internal heat flux can be much larger at the hemispheric scale than at the global scale. In fact, the hemispheric-average instantaneous internal heat flux can reach ∼100% of the emitted power during solstice seasons, comparable to the global-scale internal heat flux of other giant planets (Jupiter, Saturn, and Neptune).

Taking internal heat flux into account provides a more complete picture of the energy budget for Uranus' weather layer. The energy budget of Uranus exhibits significant imbalances at both global and hemispheric scales. In particular, the hemispheric-average energy budget shows an extreme energy excess of 95.0% ± 5.4% of the emitted power at the summer solstice and a strong energy deficit of −87.7% ± 3.9% at the winter solstice in each hemisphere. These extreme hemispheric-scale energy imbalances are primarily due to Uranus' unique axial tilt (97.7°). While numerical models (e.g., Bézard, 1990; Bezard & Gautier, 1985; Conrath et al., 1990; Friedson & Ingersoll, 1987; Milcareck et al., 2024; Wallace, 1983) have greatly advanced our understanding of Uranus' atmospheric system, some key observational characteristics (e.g., tropical warming in the upper troposphere) remain poorly simulated. A more complete picture of the energy budget may provide new insights for future numerical modeling efforts.

While current investigations help us better understand Uranus' REB and internal heat flux, more fundamental questions remain unanswered. For example, the meridional distribution of the REB, which plays a critical role in the large-scale circulation of planetary atmospheres, has not yet been determined for Uranus. Ground-based telescopes and Earth-orbiting observatories can observe Uranus' Earth-facing hemisphere, but these observations are generally limited in viewing geometry and latitude coverage. More importantly, the great distance between Earth and Uranus results in poor spatial resolution, making it difficult to resolve the planet's meridional energy distribution. On the other hand, the only flyby observations conducted by Voyager occurred near the summer solstice of the SH, providing only a very limited sunlit view of the NH. Additionally, the spectral coverage of the Voyager instruments was limited. As a result, the Voyager observations had a restricted capability to examine Uranus' meridional energy distribution. The Uranus orbiter mission recommended by the recent decadal survey presents a valuable opportunity to investigate the planet's REB and its spatiotemporal variability. By carefully selecting observation wavelengths and planning the spacecraft's orbit, this flagship mission will not only help answer fundamental questions about Uranus' REB but also significantly advance our understanding of other aspects of this ice giant.

Data Availability Statement

All data sets analyzed in this study are published and publicly available from Showalter & Gordon, 2011 (https://doi.org/10.17189/1519389) and Wenkert, 2023 (https://doi.org/10.17189/t2r8-rk88).

Acknowledgments
We would like to thank Drs. Erich Karkoschka and Daniel Wenkert for providing Earth-based and Voyager 1 data on Uranus, respectively. L.L. acknowledges support from the National Science Foundation (Grant AST-2108018) and the NASA Cassini Data Analysis & Frontier Data Analysis programs (Grants 80NSSC20K0479 and 80NSSC21K0824). X.Z. acknowledges support from the National Science Foundation Grant AST2307463 and the NASA Interdisciplinary Consortia for Astrobiology Research (ICAR) Grant 80NSSC21K0597.

References

Allison, M., Beebe, R. F., Conrath, B. J., Hinson, D. P., & Ingersoll, A. P. (1991). Uranus atmospheric dynamics and circulation. In *Uranus*. The University of Arizona Press.

Allison, M., & Travis, L. D. (1986). Astronomical, physical, and meteorological parameters for planetary atmospheres. In *The jovian atmospheres* (Vol. 2441). NASA Conference Publication.

Bézard, B. (1990). Seasonal thermal structure of the atmospheres of the giant planets. *Advances in Space Research*, *10*(1), 89–98. https://doi.org/10.1016/0273-1177(90)90091-d

Bezard, B., & Gautier, D. (1985). A model of the spatial and temporal variation of the Uranus thermal structure. In *The jovian atmospheres* (Vol. 2441). NASA Conference Publication.

Clauser, C. (2021). Radiogenic heat production of rocks. In *Encyclopedia of solid earth geophysics*. Springer International Publishing.

Conrath, B. J., Gierasch, P. J., & Leroy, S. S. (1990). Temperature and circulation in the stratosphere of the outer planets. *Icarus*, *83*(2), 255–281. https://doi.org/10.1016/0019-1035(90)90068-k

Conrath, B. J., Hanel, R. A., & Samuelson, R. E. (1989). Thermal structure and heat balance of the outer planets. In *Origin and evolution of planetary and satellite atmospheres*. The University of Arizona Press.

Flasar, F. M. (1973). Gravitational energy sources in Jupiter. *The Astrophysical Journal*, *186*, 1097–1106. https://doi.org/10.1086/152574

Friedson, J., & Ingersoll, A. P. (1987). Seasonal meridional energy balance and thermal structure of the atmosphere of Uranus: A radiative-convective-dynamical model. *Icarus*, *69*(1), 135–156. https://doi.org/10.1016/0019-1035(87)90010-8

Ge, H., Li, C., Zhang, X., & Moeckel, C. (2024). Heat-flux-limited cloud activity and vertical mixing in giant planet atmospheres with an application to Uranus and Neptune. *The Planetary Science Journal*, *5*(4), 101. https://doi.org/10.3847/psj/ad0ed3

Guillot, T. (2005). The interiors of giant planets: Models and outstanding questions. *Annual Review of Earth and Planetary Sciences*, *33*(1), 493–530. https://doi.org/10.1146/annurev.earth.32.101802.120325

Gulkis, S., & de Pater, I. (1984). A review of the millimeter and centimeter observations of Uranus. In *Uranus and Neptune* (Vol. 2330). NASA Conference Publication.

Hammel, H. B., & Lockwood, G. W. (2007). Long-term atmospheric variability on Uranus and Neptune. *Icarus*, *186*(1), 291–301. https://doi.org/10.1016/j.icarus.2006.08.027

Hanel, R., Conrath, B., Flasar, F. M., Kunde, V., Maguire, W., Pearl, J., et al. (1986). Infrared observations of the Uranian system. *Science*, *233*(4759), 70–74. https://doi.org/10.1126/science.233.4759.70

Hanel, R. A., Conrath, B. J., Jennings, D. E., & Samuelson, R. E. (2003). *Exploration of the solar system by infrared remote sensing*. Cambridge University Press.

Hubbard, W. B. (1968). Thermal structure of Jupiter. *The Astrophysical Journal*, *152*, 745–754. https://doi.org/10.1086/149591

Hubbard, W. B. (1978). Comparative thermal evolution of Uranus and Neptune. *Icarus*, *35*(2), 177–181. https://doi.org/10.1016/0019-1035(78)90002-7

Hubbard, W. B. (1980). Intrinsic luminosities of the Jovian planets. *Reviews of Geophysics*, *18*, 1–9. https://doi.org/10.1029/rg018i001p00001

Ingersoll, A. P. (1990). Atmospheric dynamics of the outer planets. *Science*, *248*(4953), 308–315. https://doi.org/10.1126/science.248.4953.308

Irwin, P. G., Dobinson, J., James, A., Teanby, N. A., Simon, A. A., Fletcher, L. N., et al. (2024). Modelling the seasonal cycle of Uranus' color and magnitude, and comparison with Neptune. *Monthly Notices of the Royal Astronomical Society*, *527*(4), 11521–11538. https://doi.org/10.1093/mnras/stad3761

Irwin, P. G. J., Teanby, N. A., Davis, G. R., Fletcher, L. N., Orton, G. S., Tice, D., & Kyffin, A. (2011). Uranus' cloud structure and seasonal variability from Gemini-North and UKIRT observations. *Icarus*, *212*(1), 339–350. https://doi.org/10.1016/j.icarus.2010.12.018

Karkoschka, E. (2001). Uranus' apparent seasonal variability in 25 HST filters. *Icarus*, *151*(1), 84–92. https://doi.org/10.1006/icar.2001.6599

Li, L., Jiang, X., West, R. A., Gierasch, P. J., Perez-Hoyos, S., Sanchez-Lavega, A., et al. (2018). Less absorbed solar energy and more internal heat for Jupiter. *Nature Communications*, *9*(1), 3709. https://doi.org/10.1038/s41467-018-06107-2

Lockwood, G. W. (1978). Analysis of photometric variations of Uranus and Neptune since 1953. *Icarus*, *35*(1), 79–92. https://doi.org/10.1016/0019-1035(78)90062-3

Lockwood, G. W. (2019). Final compilation of photometry of Uranus and Neptune, 1972–2016. *Icarus*, *324*, 77–85. https://doi.org/10.1016/j.icarus.2019.01.024

Lockwood, G. W., & Jerzykiewicz, M. (2006). Photometric variability of Uranus and Neptune, 1950–2004. *Icarus*, *180*(2), 442–452. https://doi.org/10.1016/j.icarus.2005.09.009

Malamud, U., Podolak, M., Podolak, J. I., & Bodenheimer, P. H. (2024). Uranus and Neptune as methane planets: Producing icy giants from refractory planetesimals. *Icarus*, *421*, 116217. https://doi.org/10.1016/j.icarus.2024.116217

Marley, M. S., & McKay, C. P. (1999). Thermal structure of Uranus' atmosphere. *Icarus*, *138*(2), 268–286. https://doi.org/10.1006/icar.1998.6071

Milcareck, G., Guerlet, S., Montmessin, F., Spiga, A., Leconte, J., Millour, E., et al. (2024). Radiative-convective models of the atmospheres of Uranus and Neptune: Heating sources and seasonal effects. *Astronomy & Astrophysics*, *686*, A303. https://doi.org/10.1051/0004-6361/202348987

National Academies of Sciences, Engineering, and Medicine. (2022). *Origins, worlds, and life: A decadal Strategy for planetary science and Astrobiology 2023-2032*. The National Academies Press.

Orton, G. S., Fletcher, L. N., Encrenaz, T., Leyrat, C., Roe, H. G., Fujiyoshi, T., & Pantin, E. (2015). Thermal imaging of Uranus: Upper-tropospheric temperatures one season after voyager. *Icarus*, *260*, 94–102. https://doi.org/10.1016/j.icarus.2015.07.004

Pearl, J. C., & Conrath, B. J. (1991). The albedo, effective temperature, and energy balance of Neptune, as determined from Voyager data. *Journal of Geophysical Research*, *96*(S01), 18921–18930. https://doi.org/10.1029/91ja01087

Pearl, J. C., Conrath, B. J., Hanel, R. A., Pirraglia, J. A., & Coustenis, A. (1990). The albedo, effective temperature, and energy balance of Uranus, as determined from Voyager IRIS data. *Icarus*, *84*(1), 12–28. https://doi.org/10.1016/0019-1035(90)90155-3

Podolak, M., Hubbard, W. B., & Stevenson, D. J. (1991). Models of Uranus' interior and magnetic field. *Uranus*, *1*, 29–61.

Pollack, J. B., Rages, K., Baines, K. H., Bergstralh, J. T., Wenkert, D., & Danielson, G. E. (1986). Estimates of the bolometric albedos and radiation balance of Uranus and Neptune. *Icarus*, *65*(2–3), 442–466. https://doi.org/10.1016/0019-1035(86)90147-8

Rages, K. A., Hammel, H. B., & Friedson, A. J. (2004). Evidence for temporal change at Uranus' South pole. *Icarus*, *172*(2), 548–554. https://doi.org/10.1016/j.icarus.2004.07.009

Roman, M. T., Fletcher, L. N., Orton, G. S., Rowe-Gurney, N., & Irwin, P. G. (2020). Uranus in northern midspring: Persistent atmospheric temperatures and circulations inferred from thermal imaging. *The Astronomical Journal*, *159*(2), 45. https://doi.org/10.3847/1538-3881/ab5dc7

Salpeter, E. (1973). On convection and gravitational layering in Jupiter and stars of low mass. *Astrophysica Norvegica*, *181*, L83–L86. https://doi.org/10.1086/181190

Showalter, M. R., & Gordon, M. K. (2011). Cassini Saturn composite infrared spectrometer reformatted data [Dataset]. *NASA Planetary Data System. CO-SCIRS-2/3/4-REFORMATTED-V1.0*. https://doi.org/10.17189/1519389

Smoluchowski, R. (1967). Internal structure and energy emission of Jupiter. *Nature*, *215*(5102), 691–695. https://doi.org/10.1038/215691a0

Stevenson, D. J., & Salpeter, E. E. (1977). The dynamics and helium distributions in hydrogen-helium planets. *The Astrophysical Journal–Supplement Series*, *35*, 239–261. https://doi.org/10.1086/190479

Wallace, L. (1983). The seasonal variation of the thermal structure of the atmosphere of Uranus. *Icarus*, *54*(1), 110–132. https://doi.org/10.1016/0019-1035(83)90073-8

Wang, X., Li, L., Jiang, X., Fry, P. M., West, R. A., Nixon, C. A., et al. (2024). Cassini spacecraft reveals global energy imbalance of Saturn. *Nature Communications*, *15*(1), 5045. https://doi.org/10.1038/s41467-024-48969-9

Wenkert, D. (2023). Restoring and archiving voyager 1 cruise images of Uranus and Neptune (RAV1CIUN) PDART bundle [Dataset]. *NASA Planetary Data System*. https://doi.org/10.17189/t2r8-rk88

West, R. A., Baines, K. H., & Pollack, J. B. (1991). Clouds and aerosols in the Uranian atmosphere. In *Uranus*. The University of Arizona Press.